

## Structure and Bonding of Bis(fulvalene)nickel

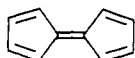
Paul R. Sharp, Kenneth N. Raymond,\*<sup>1</sup> James C. Smart,<sup>2</sup> and Ronald J. McKinney<sup>3</sup>

Contribution from the Department of Chemistry, University of California, Berkeley, California 94720, and the Central Research and Development Department, Experimental Station, E. I. du Pont de Nemours and Company, Wilmington, Delaware 19898.  
Received April 18, 1980

**Abstract:** The solid-state structure of bis(fulvalene)nickel has been determined by single-crystal X-ray diffraction methods. The compound conforms to the centrosymmetric space group  $P2_1/n$  and is isomorphous with bis(fulvalene)diiron. Unlike bis(fulvalene)diiron the C-C bond distances in the fulvalene unit are not equal but instead show localization of multiple C-C bonds similar to that of the neutral olefin. Also, inequivalence within the Ni-C bonds results from displacement of the Ni atoms from the centers of the rings and away from each other along the Ni-Ni axis. Semiempirical molecular orbital calculations have reproduced and explained the differences between the iron and nickel complexes, and some predictions are made about the structure and bonding of related species in this series. The structure was refined by full-matrix least-squares methods to final weighted and unweighted  $R$  factors of 0.037 and 0.049, respectively. Data were collected on an automated diffractometer to a Bragg  $2\theta$  scattering angle of  $55^\circ$ . The data gave 1190 averaged, unique observations with  $F^2 \geq 3\sigma(F^2)$ .

## Introduction

A major interest in the chemistry of fulvalene-metal complexes



continues to be the degree to which the adjacent metal centers coordinated by the two linked, five-membered rings are electronically coupled. Several fulvalene complexes of Ti are diamagnetic or weakly paramagnetic despite formal 17-e counts about each metal.<sup>4</sup> The diamagnetism has been ascribed to a Ti-Ti bond,<sup>5,6</sup> strong superexchange through bridging ligands,<sup>6</sup> or coupling of the metal atoms via the fulvalene ligand.<sup>4</sup> The preparation of the diamagnetic binary fulvalene complexes (Figure 1)  $\text{BFFe}^{2+}$ ,<sup>7</sup>  $\text{BFCo}^0$ ,<sup>8</sup>  $\text{BFNi}^{0,9}$  and  $\text{BFNi}^{2+9}$  has also indicated possible coupling via the fulvalene ligand since the mononuclear metallocene counterparts  $(\text{C}_5\text{H}_5)_2\text{Fe}^+$ ,  $(\text{C}_5\text{H}_5)_2\text{Co}$ ,  $(\text{C}_5\text{H}_5)_2\text{Ni}$ , and  $(\text{C}_5\text{H}_5)_2\text{Ni}^+$  are paramagnetic. While the crystal structure of  $(\text{C}_{10}\text{H}_8)_2\text{Fe}_2$ <sup>10</sup> revealed a ferrocene-like geometry about each iron atom, the above observations led us to undertake a detailed single-crystal X-ray diffraction study of  $(\text{C}_{10}\text{H}_8)_2\text{Ni}_2$  in the hope of observing structural deviations which could account for its diamagnetism. Subsequently, semiempirical molecular orbital calculations were carried out in order to rationalize these findings and provide a basis for the systematic prediction of the changes in the structure and bonding of members of this structural series accompanying addition or removal of electrons.

## Experimental Section

**Crystal Growth, Characterization, and Data Collection.** A sample of  $(\text{C}_{10}\text{H}_8)_2\text{Ni}_2$  was supplied by B. Pinsky.<sup>9</sup> Suitable crystals were grown by slow cooling of a hot, saturated mesitylene solution under  $\text{N}_2$ . The crystals could be handled in the air without noticeable decomposition for

Table I. Crystal Data and Intensity Data Collection Summary

mol formula	$\text{Ni}_2\text{C}_{20}\text{H}_{16}$
mol wt	373.77
space group	$P2_1/n$ , <sup>a</sup> monoclinic
formulas/cell	2
$a$ , Å	9.430 (2)
$b$ , Å	7.752 (2)
$c$ , Å	10.628 (2)
$\beta$ , deg	109.76 (1)
cell V, Å <sup>3</sup>	731.22
calcd density, g/cm <sup>3</sup>	1.69
obsd density (floatation), g/cm <sup>3</sup>	1.71 (2)
linear abs coeff., cm <sup>-1</sup>	25.54
abs cor range	1.36-1.61
crystal size, cm	$0.022 \times 0.014 \times 0.013$
data collected	$\pm h, k, l$ to $2\theta = 55^\circ$ , $\pm h, -k, l$ and $\pm h, k, -l$ to $2\theta = 50^\circ$
scan rate	1°/min
Bkgd time	10s
$2\theta$ scan width (at $2\theta = 0$ )	1.6°
radiation	Mo $K\alpha_1$ , $\lambda = 0.709261$ Å
final no. of data and parameters in refinement	1190 data 132 parameters
$R^b$	4.92%
$R_w$	3.67%

<sup>a</sup> See footnote 11. <sup>b</sup> See footnote 18.

at least 24 h but as a precaution were mounted in glass capillaries or on glass rods and coated with acrylic polymer. Precession and Weissenberg photographs exhibited Laue symmetry,  $2/m$  and absences  $h0l$ ,  $h + l = 2n + 1$  and  $0k0$ ,  $k = 2n + 1$ , leading to the unambiguous assignment of the centrosymmetric space group  $P2_1/n$ .<sup>11</sup>

Intensity data were collected by the  $\theta$ - $2\theta$  scan technique with a Picker FACS-1 four-circle diffractometer at ambient temperature of  $24^\circ\text{C}$ . The data crystal was judged to be of good quality on the basis of  $\omega$  scans of several intense reflections with half-peak-height widths of  $<0.1^\circ$ . Determination of lattice parameters, collection of intensity data, and processing of the data were performed as previously described.<sup>12</sup> Experimental parameters along with pertinent crystal data are presented in Table I. Absorption corrections were made by an analytical integration method,<sup>13</sup> after which equivalent reflections were averaged and

(1) To whom correspondence should be addressed at the University of California.

(2) Research Division, Solar Energy Research Institute, 1536 Cole Boulevard, Golden, Colorado 80401.

(3) Central Research and Development Department, E. I. du Pont de Nemours and Co. (contribution No. 2748).

(4) Olthof, G. J. *J. Organomet. Chem.* **1977**, *128*, 367 and references therein.

(5) Salzmann, J. J.; Mosimann, P. *Helv. Chim. Acta* **1967**, *50*, 1831.

(6) Guggenberger, L. J.; Tebbe, F. N. *J. Am. Chem. Soc.* **1973**, *95*, 7870.

(7) Mueller-Westerhoff, U. T.; Eilbracht, P. *Tetrahedron Lett.* **1973**, *21*, 1855.

(8) Smart, J. C.; Pinsky, B. L., unpublished results.

(9) Smart, J. C.; Pinsky, B. L. *J. Am. Chem. Soc.* **1977**, *99*, 956.

(10) Churchill, M. R.; Wormald, J. *Inorg. Chem.* **1969**, *8*, 1970.

(11) A nonstandard setting of  $P2_1/c$  [ $C_{2h}^2$ ; No. 14]; equivalent positions  $\pm(x, y, z)$  and  $\pm(1/2 - x, 1/2 + y, 1/2 - z)$ .

(12) Baker, E. C.; Brown, L. D.; Raymond, K. N. *Inorg. Chem.* **1975**, *14*, 1376.

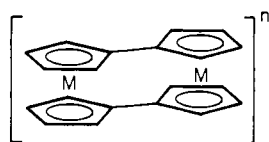
Table II. Positional, Isotropic Thermal, and Anisotropic<sup>a</sup> Thermal ( $\times 10^4$ ) Parameters<sup>b</sup>

atom	x	y	z	$\beta_{11}$	$\beta_{22}$	$\beta_{33}$	$\beta_{12}$	$\beta_{13}$	$\beta_{23}$
Ni	0.21025 (6)	0.04539 (7)	0.48304 (5)	82.4 (8)	91.9 (10)	60.3 (6)	6.7 (7)	25.0 (5)	12.9 (6)
C(1)	0.1520 (5)	-0.1521 (5)	0.6128 (4)	85 (5)	80 (6)	51 (4)	6 (5)	14 (4)	14 (4)
C(2)	0.2644 (5)	-0.0349 (6)	0.6902 (4)	107 (6)	108 (7)	62 (4)	0 (6)	13 (4)	2 (5)
C(3)	0.3909 (5)	-0.0468 (7)	0.6501 (5)	84 (6)	149 (9)	91 (6)	6 (7)	8 (5)	26 (6)
C(4)	0.3592 (6)	-0.1682 (6)	0.5437 (5)	102 (6)	121 (8)	110 (6)	39 (6)	53 (5)	19 (6)
C(5)	0.2137 (5)	-0.2312 (6)	0.5203 (5)	113 (7)	89 (7)	80 (5)	17 (6)	38 (5)	5 (5)
C(6)	-0.0070 (5)	0.1843 (5)	0.3763 (4)	102 (6)	79 (7)	67 (5)	13 (5)	36 (4)	19 (4)
C(7)	0.1056 (5)	0.2994 (6)	0.4557 (5)	107 (6)	87 (7)	92 (6)	3 (6)	38 (5)	8 (5)
C(8)	0.2291 (6)	0.2959 (6)	0.4106 (6)	120 (7)	132 (9)	121 (7)	-7 (7)	43 (6)	51 (6)
C(9)	0.1974 (6)	0.1760 (7)	0.3036 (5)	124 (7)	193 (11)	90 (6)	37 (8)	54 (5)	55 (7)
C(10)	0.0540 (6)	0.1051 (7)	0.2831 (4)	122 (7)	150 (9)	56 (5)	14 (7)	32 (5)	11 (5)

atom	x	y	z	$B, \text{\AA}^2$	atom	x	y	z	$B, \text{\AA}^2$
H(2)	0.253 (5)	0.041 (5)	0.758 (5)	3.1 (9)	H(7)	0.104 (5)	0.370 (6)	0.531 (4)	3.2 (10)
H(3)	0.483 (6)	0.008 (6)	0.683 (5)	3.4 (11)	H(8)	0.316 (6)	0.370 (7)	0.443 (5)	4.6 (12)
H(4)	0.418 (7)	-0.206 (7)	0.498 (5)	5.6 (15)	H(9)	0.266 (7)	0.154 (7)	0.254 (5)	5.0 (13)
H(5)	0.152 (5)	-0.318 (6)	0.446 (4)	3.2 (10)	H(10)	0.002 (6)	0.017 (6)	0.217 (5)	3.6 (11)

<sup>a</sup> The form of the anisotropic temperature factor is  $\exp[-\beta_{11}h^2 + \beta_{22}k^2 + \beta_{33}l^2 + 2\beta_{12}hk + 2\beta_{13}hl + 2\beta_{23}kl]$ . <sup>b</sup> Standard deviations of the last significant figures in parentheses. <sup>c</sup> For the hydrogen atoms  $B$  is the isotropic temperature factor in  $\exp(-B(\sin \theta/\lambda)^2)$ .



M = Fe, BFFe(n)  
M = Co, BFCo(n)  
M = Ni, BFNi(n)

**Figure 1.** Structural diagram of the bis(fulvalene)dimetal complexes discussed and the symbols used for each. For example, the neutral coupled ferrocene analogue, bis(fulvalene)diiron, is BFFe<sup>0</sup> while the isoelectronic cobalt dication is BFCo<sup>2+</sup>. The compound described in this paper is BFNi<sup>0</sup>.

placed upon an approximately absolute scale by the method of Wilson.<sup>14</sup>

**Structure Refinement.** Starting positional parameters were obtained from the bis(fulvalene)diiron structure.<sup>10</sup> Full-matrix least-squares refinement minimizing the function  $\sum w(F_o^2 - F_c^2)^2$  where  $w = 1/\sigma^2(F_o^2)$  and  $F_o^2 > 3\sigma(F_o^2)$  converged rapidly. Atomic scattering factors for neutral Ni and C were those tabulated by Cromer and Mann,<sup>15</sup> and those for hydrogen were as given by Stewart, Davidson, and Simpson for the bonded atom.<sup>16</sup> Corrections for the effects of anomalous dispersion by the Ni atom were made, including both the real and imaginary terms.<sup>17</sup> Near the end of anisotropic refinement a difference map readily revealed the locations of all hydrogen atoms. These were included as variables with isotropic thermal parameters in subsequent refinement. Weighted and unweighted  $R$  factors<sup>18</sup> of 0.037 and 0.049, respectively, resulted when refinement was terminated with all shifts less than  $0.1\sigma$ . The error in an observation of unit weight<sup>19</sup> was 1.74 for 1190 reflections and 132 refined parameters. A final difference map showed no features greater than  $0.8 \text{ e \AA}^{-3}$ , the larger of which were near the metal and inversion center.

Positional and thermal parameters are tabulated in Table II. Calculated and observed structure factors are available as supplementary material (see paragraph at end of paper).

**Computational Details.** Molecular orbital calculations were carried out with use of a semiempirical theory derived by A. Anderson.<sup>20</sup> The theory is related to extended Hückel theory (EHT)<sup>21</sup> but contains a

(13) (a) de Meulenaev, J.; Tompa, H. *Acta Crystallogr.* **1965**, *19*, 1014. (b) Templeton, L. K.; Templeton, D. H. "Abstracts of Papers", American Crystallographic Association Summer Meeting, Storrs, CT; June 1973; Abstract E19.

(14) Wilson, A. J. C. *Nature (London)* **1942**, *150*, 152.

(15) Cromer, D. T.; Mann, B. *Acta Crystallogr., Sect. A* **1968**, *A24*, 321.

(16) Stewart, R. F.; Davidson, E. R.; Simpson, W. T. *J. Chem. Phys.* **1965**, *42*, 3175.

(17) Cromer, D. T. *Acta Crystallogr., Sect. A* **1965**, *A18*, 17.

(18)  $R = (\sum |F_o| - |F_c|) / \sum |F_o|$ ;  $R_w = [(\sum w(|F_o| - |F_c|)^2) / \sum w|F_o|^2]^{1/2}$ .

(19) The error in an observation of unit weight, or goodness-of-fit is given by  $\text{GOF} = [(\sum w(|F_o| - |F_c|)^2) / (N_o - N_v)]^{1/2}$ , where  $N_o$  = number of observations and  $N_v$  = number of variables.

(20) Anderson, A. B. *J. Chem. Phys.* **1975**, *62*, 1187.

Table III. Important Distances ( $\text{\AA}$ ) and Angles (Deg)

Distances			
Ni-Ni	4.163 (1)	C(1)-C(6')	1.433 (6)
Ni-C(1)	2.251 (4)	C(1)-C(2)	1.427 (6)
Ni-C(6)	2.253 (4)	C(5)-C(1)	1.439 (6)
average <sup>a</sup>	2.252 (3)	C(6)-C(7)	1.425 (6)
Ni-C(2)	2.177 (4)	C(10)-C(6)	1.441 (6)
Ni-C(5)	2.180 (4)	average	1.433 (4)
Ni-C(7)	2.178 (4)	C(2)-C(3)	1.400 (7)
Ni-C(10)	2.188 (4)	C(4)-C(5)	1.397 (7)
average	2.180 (2)	C(7)-C(8)	1.402 (8)
Ni-C(3)	2.127 (4)	C(9)-C(10)	1.407 (8)
Ni-C(4)	2.126 (5)	average	1.401 (2)
Ni-C(8)	2.119 (5)	C(3)-C(4)	1.424 (7)
Ni-C(9)	2.127 (5)	C(8)-C(9)	1.420 (8)
average	2.125 (2)	average	1.422 (2)

Angles			
C(1)-Ni-C(2)	37.6 (2)	C(1)-C(2)-C(3)	109.0 (4)
C(1)-Ni-C(5)	38.9 (2)	C(1)-C(5)-C(4)	109.2 (4)
C(6)-Ni-C(7)	37.5 (2)	C(6)-C(7)-C(8)	108.9 (4)
C(6)-Ni-C(10)	37.8 (2)	C(6)-C(10)-C(9)	108.3 (5)
average	37.70 (9)	average	108.85 (19)
C(2)-Ni-C(3)	37.9 (2)	C(2)-C(3)-C(4)	108.3 (4)
C(4)-Ni-C(5)	37.8 (2)	C(5)-C(4)-C(3)	107.6 (5)
C(7)-Ni-C(8)	38.1 (2)	C(7)-C(8)-C(9)	108.2 (5)
C(9)-Ni-C(10)	38.0 (2)	C(10)-C(9)-C(8)	108.1 (5)
average	37.95 (6)	average	108.03 (19)
C(3)-Ni-C(4)	39.1 (2)	C(5)-C(1)-C(2)	105.8 (4)
C(8)-Ni-C(9)	39.1 (2)	C(19)-C(6)-C(7)	106.4 (4)
average	39.10 (14)	average	106.1 (3)
		C(2)-C(1)-C(6')	127.4 (4)
		C(5)-C(1)-C(6')	126.8 (4)
		C(7)-C(6)-C(1')	127.0 (4)
		C(10)-C(6)-C(1')	126.5 (4)
		average	126.93 (19)

<sup>a</sup> Averages are computed for distances or angles related by  $D_{2h}$  symmetry. The esd's of the averages are the larger of the experimental variance,  $\sigma^2(\bar{x}) = (\sum_{i=1}^n (x_i - \bar{x})^2) / (n(n-1))$ , or the mean variance calculated from the least-squares esd's in individual parameters  $1/[\sigma^2(\bar{x})] = \sum_{i=1}^n 1/[\sigma^2(x_i)]$ .

correction for two-body repulsions. It has been used successfully in reproducing organometallic geometries in a variety of systems.<sup>22</sup> The parameter set and optimization routines have been described previously.<sup>22c</sup>

(21) Hoffmann, R. *J. Chem. Phys.* **1963**, *39*, 1397. Hoffmann, R.; Lipscomb, W. N. *Ibid.* **1962**, *36*, 2179, 3489; *37*, 2972.

(22) (a) Anderson, A. B. *J. Am. Chem. Soc.* **1978**, *100*, 1153. (b) Anderson, A. B. *Inorg. Chem.* **1976**, *15*, 2598. (c) Pensak, D. A.; McKinney, R. J. *Ibid.* **1979**, *18*, 3407. (d) Harlow, R. L.; McKinney, R. J.; Ittel, S. D. *J. Am. Chem. Soc.* **1979**, *101*, 7496.

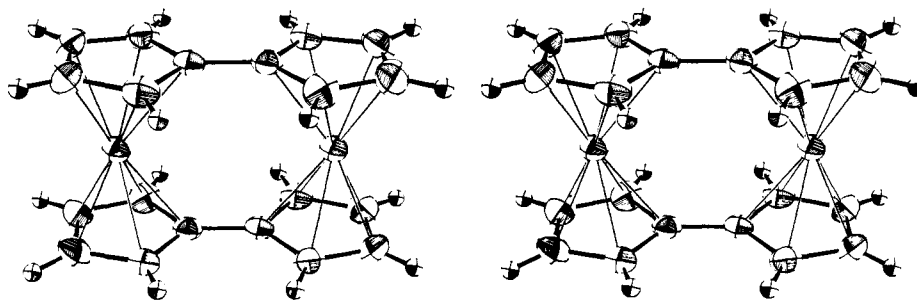


Figure 2. Stereoscopic drawing of the bis(fulvalene)nickel molecule. Anisotropic thermal parameters are represented by 50% probability ellipsoids. Hydrogen atoms are represented by spheres of arbitrary radius.

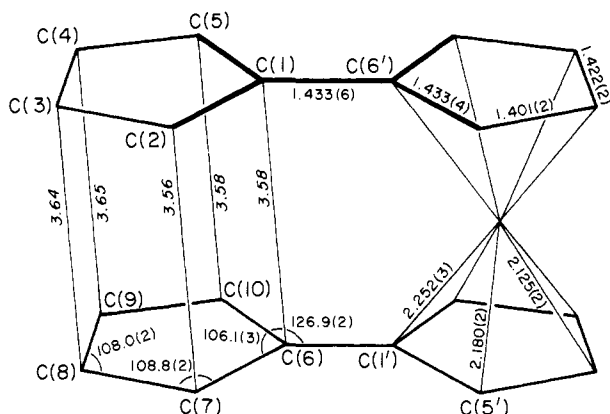


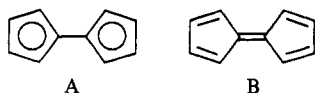
Figure 3. Atomic numbering scheme used in this paper; primed and unprimed atoms are related by the inversion center at the center of the molecule. Bond distances and angles shown are averaged with the assumption of  $D_{2h}$  molecular symmetry (see Table III).

## Results and Discussion

Bis(fulvalene)nickel [BFNi<sup>0</sup>] and bis(fulvalene)diiron [BFFe<sup>0</sup>] are isostructural as required by their isomorphous character and the successful refinement of bis(fulvalene)nickel with use of the bis(fulvalene)diiron positional parameters; a stereoscopic view of BFNi<sup>0</sup> is shown in Figure 2. However, close examination of the important bond distances and angles of bis(fulvalene)nickel in Table III reveals significant differences in the interatomic distances of the two structures.

The C-C bond distances in this structure are not all equal<sup>23</sup> but instead vary systematically while conforming to a  $D_{2h}$  point symmetry of the molecule. Since the structural features closely adhere to the ideal  $D_{2h}$  symmetry of the molecule, we deem it legitimate to average the C-C bonds related by the symmetry operations of the  $D_{2h}$  point group. Improved standard deviations result and allow division of the C-C bonds into four sets, the shortest of which is unique at 1.401 (4) and the next shortest is possibly unique at 1.422 (5) Å.<sup>23</sup> The other two sets which include the bridge bond are equal within experimental error at 1.433 (4) and 1.433 (6) Å. These results are summarized in Table III and illustrated in Figure 3. Variations in the intraring C-C bond lengths were observed in bis(fulvalene)diiron, but the differences were not systematic and not deemed significant.<sup>10</sup>

Systematic variations have been observed for the fulvalene unit in [(C<sub>10</sub>H<sub>8</sub>)(C<sub>5</sub>H<sub>5</sub>)<sub>2</sub>Ti<sub>2</sub>Cl<sub>2</sub>],<sup>24</sup> and the C-C bond distances corresponding to those of BFNi<sup>0</sup> are nearly identical. Contribution of the fulvalene resonance form B was cited as the cause of the



variations and may also apply for bis(fulvalene)nickel where

(23) Stout, G. H.; Jensen, L. H. "X-Ray Structure Determination"; Macmillan: London, 1968; pp 419-425.

(24) Olthof, G. L. *J. Organomet. Chem.* **1977**, *128*, 367.

atom	dist, Å	atom	dist, Å
Plane A: $1.5434x - 5.65624y + 6.05784z - 5.79847 = 0$			
C(1)	0.0090 (37)	C(4)	0.0009 (47)
C(2)	-0.0122 (43)	C(5)	-0.0089 (44)
C(3)	0.0075 (46)		
Plane B: $1.85953x - 5.67355y + 5.8067z - 4.67966 = 0$			
C(6)	0.0096 (38)	C(9)	0.0056 (47)
C(7)	-0.0090 (44)	C(10)	-0.0110 (45)
C(8)	0.0038 (48)		

<sup>a</sup> The equation of the plane in monoclinic coordinates is  $Ax + By + Cz - D = 0$ . See ref 29.

this structural variation is much more pronounced. [However, it will be shown later that this essentially valence-bond approach does not lead to the same predictions as a Hückel molecular orbital approach in other bis(fulvalene) complexes.]

Regular variation of the Ni-C distances in BFNi<sup>0</sup> give three sets which also have been averaged similar to the C-C distances (vide supra). These are tabulated in Table II and illustrated in Figure 3. The variation is due primarily to a displacement of the Ni atoms from the centers of their respective metallocene moieties by ca. 0.1 Å along the Ni-Ni axis toward the ends of the molecule (i.e., away from each other). The resulting Ni-Ni distance of 4.163 (1) Å is considerably greater than the Fe-Fe distance of 3.984 (4) Å found in bis(fulvalene)diiron and definitely excludes any direct Ni-Ni bonding interaction. Such a displacement would seem consistent with contribution of the fulvalene resonance form B and perhaps a more correct formulation of bis(fulvalene)nickel as a Ni(0) polyolefin complex, which should be diamagnetic.

The rigidity of the fulvalene unit makes comparison of the Ni-C distances with those of Ni(0)-olefin complexes difficult at best. Average Ni-C distances in simple Ni(0)-olefin complexes range from 1.91 to 2.02 Å,<sup>25</sup> shorter than any of the Ni-C distances observed here. However, in the more rigid bis(cyclooctadiene)nickel, the average Ni-C distance is 2.12 (1) Å,<sup>26</sup> essentially identical with the shortest average distance of 2.125 (2) Å in bis(fulvalene)nickel. A comparison with a different formal oxidation state can be made by noting that this distance also falls within the range of 2.11-2.15 Å observed for monocyclopentadienylnickel(II) complexes.<sup>27</sup> A longer distance of 2.196 (8) Å was found for nickelocene by electron diffraction<sup>28</sup> and is close to the average Ni-C distance of 2.180 (2) Å found for the central carbons [C(5), etc.]. The average Ni-C distance (at the bridgehead carbon atoms [C(1) and C(6)], 2.252 (3) Å, is, to our knowledge, the longest Ni-C distance reported. This indicates

(25) Brauer, D. J.; Kruger, C. *J. Organomet. Chem.* **1974**, *77*, 423. Guggenberger, L. *J. Inorg. Chem.* **1973**, *12*, 499. Ibers, J. A.; Ittel, S. *Adv. Organomet. Chem.* **1976**, *14*, 33 and references cited therein.

(26) Dierks, H.; Dietrich, H. *Z. Kristallogr., Kristallgeom. Kristallphys., Kristallchem.* **1965**, *122*, 1.

(27) Wong, Y.; Coppens, P. *Inorg. Chem.* **1976**, *15*, 1122. Adams, R. D.; Cotton, F. A.; Rusholme, G. A. *J. Coord. Chem.* **1971**, *1*, 275. Churchill, M. R.; O'Brian, T. A. *J. Chem. Soc. A* **1970**, 161; **1969**, 266; **1968**, 2970. Miller, O.S.; Shaw, B. W. *J. Organomet. Chem.* **1968**, *11*, 595. Dahl, L. F.; Wei, G. W. *Inorg. Chem.* **1963**, *2*, 713.

(28) Hedberg, L.; Hedberg, K. *J. Chem. Phys.* **1970**, *53*, 1228.

Table V. Comparison of Calculated and Observed Geometries

	Fe		Co		Ni	
	calcd	obsd <sup>c</sup>	calcd	calcd	obsd	
$x^a$	3.92	3.98	4.08	4.19	4.16	
$y^b$	3.39		3.48	3.61	3.60	
M-C(1)	2.09	2.05	2.18	2.26	2.25	
M-C(2)	2.09	2.05	2.15	2.21	2.18	
M-C(3)	2.09	2.05	2.10	2.13	2.13	

<sup>a</sup> Metal-metal distance. <sup>b</sup> Distance between fulvalene ligands.  
<sup>c</sup> Reference 10.

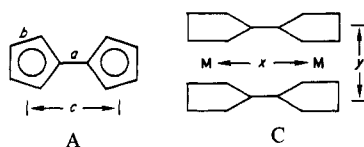
a weak interaction of the metal with the bridgehead carbon atoms, which again supports the contribution of the fulvalene resonance form B.

Some distortion of the fulvalene ring was found in the non-planarity<sup>23,29</sup> of the individual five-membered ring systems (Table IV). The distortion is best viewed by examining the inter-ring C-C distances (Figure 3). The inside three sets, C(1)-C(6), C(2)-C(7), and C(5)-C(10), are nearly equal, whereas the outer two, C(3)-C(8) and C(4)-C(9), are about 0.08 Å longer—indicating an outward tilt at the end of the rings. Note that the two longer C-C inter-ring distances are between the carbons with the shortest Ni-C distances.

All other features of the molecule are "normal". The ring carbon angles have some spread [105.8 (4)–109.2 (4)], with the bridgehead carbons C(1) and C(6) having the two smallest values. The thermal ellipsoids are of reasonable size and orientation, the minor axes being oriented approximately along the Ni-C direction. The C-H distances are all close to their average of 0.97 (2) Å, which agrees well with the accepted value of 0.95 Å for X-ray diffraction measurements.<sup>30</sup>

### Theoretical Results

Semiempirical molecular orbital<sup>20,22</sup> calculations were carried out for the model complexes A and C. The bond distances and



angles of the fulvalene ligands (A) were held constant such that the C<sub>5</sub> rings kept pentagonal symmetry (all C-C distances equal and all C-C-C interior angles = 108°) with  $a = 1.46$ ,  $b = 1.44$ , and  $c = 3.92$  Å. In the fulvalene complex C the distances between metals and fulvalene ligands ( $y$ ) were varied within  $D_{2h}$  symmetry constraints to obtain the lowest energy geometry. We used cobalt for the metal and either removed or added two electrons to model the iron and nickel cases, respectively. The results of computational optimization (Table V) are in remarkable agreement with the X-ray structural results for the iron and nickel complexes. For the nickel complex, the overall geometry was reproduced in spite of not allowing the skeleton of the fulvalene ligands to change. In fact, using the observed ligand geometry resulted in insignificant differences in the parameters  $x$  and  $y$  upon reoptimization. The calculations suggest that the position of cobalt with respect to the ring centroids will be intermediate between that found for the iron and that for the nickel complexes.

Since fulvalene C-C distances were held constant while the metal positions were varied, changes in the Mulliken overlap population analysis should reflect observed changes in C-C bond distances. For the iron complex, the overlap population between C(1)-C(2), (1.21), C(2)-C(3) (1.22), and C(3)-C(4) (1.22) are similar—as expected for a ferrocene-type structure. However, for the nickel complex the respective overlap populations are 1.17, 1.22, and 1.21, suggesting that the bond lengths should decrease in the order C(1)-C(2) > C(3)-C(4) ≥ C(2)-C(3), consistent with the observed systematic bond differences (1.43, 1.42, and

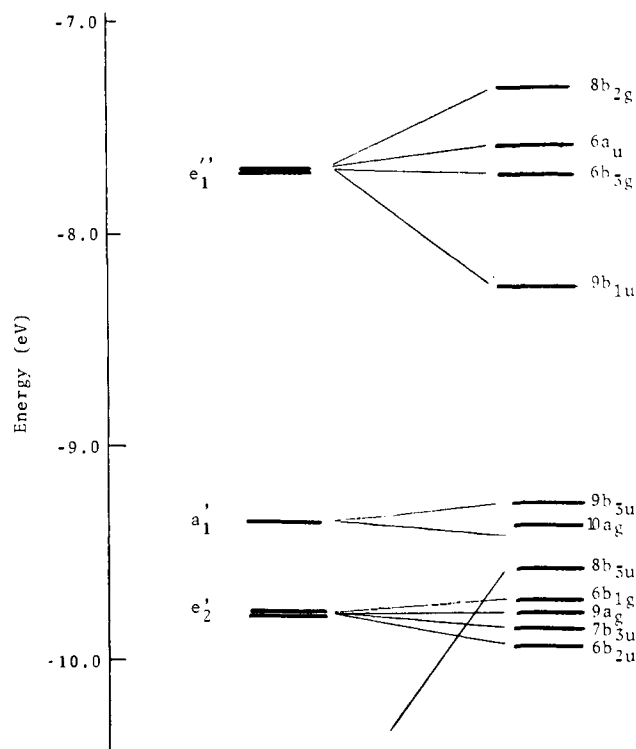
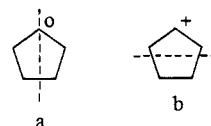


Figure 4. Qualitative energy level diagram for bis(fulvalene)dimetal.

1.40 Å, respectively). For the cobalt complex, it is suggested that there is bond-length variation in the order C(1)-C(2) > C(2)-C(3) > C(3)-C(4) (populations of 1.18, 1.21, and 1.23, respectively). The overlap populations for C(1)-C(6') (Fe, 1.04; Co, 1.08; Ni, 1.06) are consistent with the observed shortening in going from the iron to nickel complex and also suggest that the bond in the cobalt complex will be shorter still. The latter prediction is not made by a simple consideration of the valence-bond resonance structures. The overlap population of C(1)-C(6') cannot be meaningfully compared with intra-ring C-C populations because they are calculated at different distances. The same trends are observed when only the carbon  $\pi\pi$  overlaps are examined.

The calculated and observed differences between the iron and nickel complexes may be rationalized by examining the nature of the two molecular orbitals which are successively filled in progressing from iron to cobalt to nickel. These orbitals,  $9b_{1u}$  and  $6b_{3g}$  in Figure 4, result from the interaction of what would be the  $e_1''$  (antibonding) orbitals of isolated  $D_{5h}$  metallocene units and include some contribution of the metal  $d_{xz}$  and  $d_{yz}$  orbitals. The  $e_1''$  orbitals can be written as an orthogonal pair in which one orbital has a nodal plane passing through a carbon atom (a) and



the second orbital has a large coefficient on the same carbon atom (b), as shown for one C<sub>5</sub> ring of each metallocene unit. Bringing two such C<sub>5</sub> units together at the carbon atoms through which the nodal plane passes in a results in the  $a \pm a$  combinations  $6b_{3g}$  and  $6a_{1u}$ , which are weakly split in energy relative to the  $e_1''$  orbitals. In contrast, strong splitting results from interaction of  $b \pm b$  to give the  $9b_{1u}$  and  $8b_{2g}$  orbitals. While changes in geometry and electron count cause some variation in energy levels, no orbital crossings result, and therefore the energy level diagram in Figure 4 may be used qualitatively for the iron, cobalt, and

(29) Hamilton, W. C. *Acta Crystallogr.* 1961, 14, 185.

(30) Churchill, M. R. *Inorg. Chem.* 1973, 12, 1213.

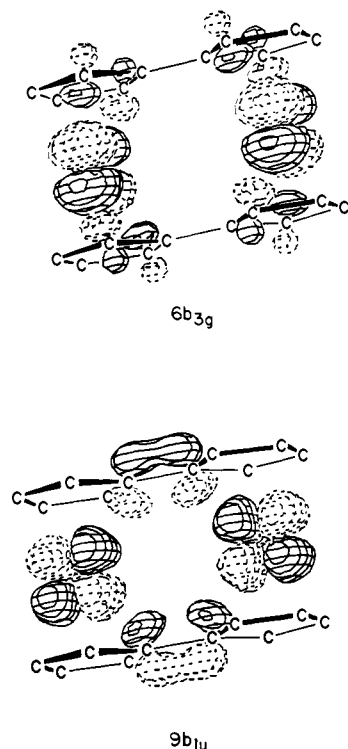
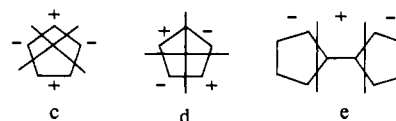


Figure 5. Molecular orbital envelopes for the HOMO's of bis(fulvalene)dinickel ( $6b_{3g}$ ) and bis(fulvalene)dnicobalt ( $9b_{1u}$ ), respectively.

nickel cases. Our calculations are consistent with the calculations of Kirchner, Loew, and Mueller-Westerhoff,<sup>31</sup> who have described the nature of the frontier orbitals of bis(fulvalene)diiron.

The  $9b_{1u}$  and  $6b_{3g}$  orbitals, illustrated in Figure 5, are occupied in the nickel complex but not in the iron complex and therefore should reflect the observed geometrical changes. The  $9b_{1u}$  orbital is antibonding between metal and fulvalene ligand, causing an increase in the metal-metal and metal-fulvalene distances, and bonding between C(1)-C(6'), causing a shortening of the bond. The  $6b_{3g}$  orbital is again antibonding between metal and fulvalene, causing a further increase in distance. In addition to the interactions illustrated in Figure 5, the wave-function coefficients reveal that the  $9b_{1u}$  orbital has small antibonding contributions between C(1)-C(2) and C(1)-C(5) and small bonding contributions between C(2)-C(3) and C(4)-C(5). This appears to conflict with

the assignment of the  $9b_{1u}$  orbital as a  $b + b$  combination. The position of the nodal planes as shown in b would result in bonding between C(1)-C(2) and antibonding between C(2)-C(3). However, in the  $D_{5h}$  metallocene, the higher energy  $e_2''$  orbitals, represented by the orthogonal pair c and d, may combine to give c



$\pm c$  [ $10b_{1u}$  and  $11a_g$ ] and  $d \pm d$  [ $7b_{3g}$  and  $7a_u$ ]. Because the  $b + b$  and  $c + c$  combinations are of the same symmetry ( $b_{1u}$ ), b and c may now mix, which results in an effective shift of the nodal planes so that the nodal planes of the  $9b_{1u}$  orbital may be represented as in e. The reason for lengthening C(1)-C(2) and shortening C(2)-C(3) upon occupation of this orbital now becomes apparent. The  $6b_{3g}$  orbital has small bonding contributions between C(2)-C(3) and C(4)-C(5) and small antibonding contributions for C(3)-C(4) which are consistent with the nodal structure of a. The occupation of these orbitals therefore accounts for the systematic changes observed in the fulvalene ligands of the nickel complex.

Finally, the observed diamagnetism of the three complexes discussed here, especially the cobalt and nickel complexes, has been the cause of some controversy. The relatively large HOMO-LUMO gap in the iron complex ( $9b_{3u} \rightarrow 9b_{1u}$ ) is consistent with the spin-paired ground-state configuration. The narrower HOMO-LUMO gap for the cobalt complex ( $9b_{1u} \rightarrow 6b_{3g}$ ) could be argued either for or against a spin-paired ground-state configuration. In contrast, the very narrow HOMO-LUMO gap illustrated for the nickel complex ( $6b_{3g} \rightarrow 6a_u$ ) would strongly suggest a spin-unpaired ground-state configuration. However, one must remember that when a number of low-lying unfilled orbitals exist, configuration interaction (CI) must be considered. One can quickly determine that a number of relatively low energy configurations give rise to  $A_g$  electronic states. For example, a configuration in which the  $9b_{1u}$ ,  $6b_{3g}$ ,  $6a_u$ , and  $8b_{2g}$  orbitals are singly occupied transforms as an  $A_g$  state, which will interact with, and lower the energy of, the spin-paired  $A_g$  state. Considering the observed diamagnetism of these complexes, the lowering in energy is evidently sufficient to make the spin-paired configuration the ground state.

**Acknowledgment.** P.R.S. thanks Dr. F. R. Fronczek for many helpful discussions. We thank Dr. B. L. Pinsky for providing samples of the compounds he prepared.

**Supplementary Material Available:** A listing of structure factor amplitudes (9 pages). Ordering information is given on any current masthead page.

(31) Kirchner, R. F.; Loew, G. H.; Mueller-Westerhoff, U. T. *Inorg. Chem.* **1976**, *15*, 2665.